Protoplasma (2002) 219: 160–167

PROTOPLASMA

Fasting induces cyanide-resistant respiration and oxidative stress in the amoeba *Chaos carolinensis*: implications for the cubic structural transition in mitochondrial membranes

Yuru Deng[1], **Sepp D. Kohlwein**[2], and **Carmen A. Mannella**[1,*]

[1] Wadsworth Center, New York State Department of Health, Albany, New York
[2] Biomembrane Special Research Center, Department of Molecular Biology, Biochemistry and Microbiology, University of Graz, Graz

Received September 1, 2001
Accepted January 7, 2002

Summary. Large free-living amoeba (*Chaos carolinensis*) can survive in spring water without food intake for several weeks. Starvation is associated with a dramatic change in mitochondrial cristae from random tubular to ordered (paracrystalline) cubic morphology. Whole-cell polarography was used to monitor changes in respiratory activity during fasting. Basal respiration per cell decreased progressively during starvation, while the cyanide-resistant fraction increased. Spectrofluorometric assay of H_2O_2 and reactive oxygen species (ROS) in cell lysates (using the dye 2′,7′-dichlorofluorescein diacetate) indicates greater H_2O_2 and ROS generation in starved than in fed cells. Fluorescence microscopy of intact cells incubated with the same dye demonstrates that H_2O_2 and ROS tend to accumulate in vacuoles. A remarkable generation of O_2 observed with starved cells after addition of KCN may be explained by release of H_2O_2 from these compartments into the cytosol, where it can react with catalase. Together, these observations suggest that fasting increases oxidative stress in the amoeba and that this organism has several protective mechanisms to deal with it, including activation of a plantlike alternative oxidase. The hypothesis is forwarded that the cubic structural transition of the mitochondrial inner membrane represents another protective mechanism, reducing oxidative damage by enhancing the efflux of H_2O_2 and ROS and by reducing the susceptibility of membrane lipids to the oxidants.

Keywords: Cubic phase; Mitochondrial crista; Cyanide-resistant respiration; Reactive oxygen species; Oxidative stress; Lipid peroxidation.

Abbreviations: ROS reactive oxygen species; AOX alternative oxidase; SHAM salicyl hydroxamate; H_2DCF-DA 2′,7′-dichlorofluorescein diacetate.

* Correspondence and reprints: Wadsworth Center, Empire State Plaza, Box 509, Albany, NY 12201-0509, U.S.A.
E-mail: carmen@wadsworth.org

Introduction

Cubic membranes are symmetric, periodic structures that occur in a wide variety of living systems (Landh 1995, 1996). They are based on the highly curved cubic surface and are mathematically analogous to triply periodic minimal surfaces used in describing both crystalline and liquid crystalline materials at a variety of length scales (Hyde 1996). The convoluted bilayers of cubic membrane systems extend periodically in three dimensions, creating two discrete networks of water channels (Larsson 1989). The reversed cubic phase is also a popular candidate for drug delivery due to its amphiphilic character, its highly ordered structure, and its ability to incorporate various proteins (Engström 1990). To date, three types of cubic membrane morphologies (gyroid, double diamond, and primitive) have been identified in both synthetic lipid mixtures and natural biomembranes (Landh 1996). However, the mechanisms of formation and maintenance of cubic membranes and their function in living cells remains an enigma.

It is well known that the shape of mitochondrial cristae can change with physiological conditions (e.g., Munn 1974). Mitochondrial cristae in the free-living, giant amoeba *Chaos carolinensis* undergo a dramatic change during fasting, from random tubular to an ordered morphology, starting within 1 day of fasting and increasing in frequency over time (Daniel and Breyer 1968). Through simulation of transmission electron microscopic projections (Deng and Miec-

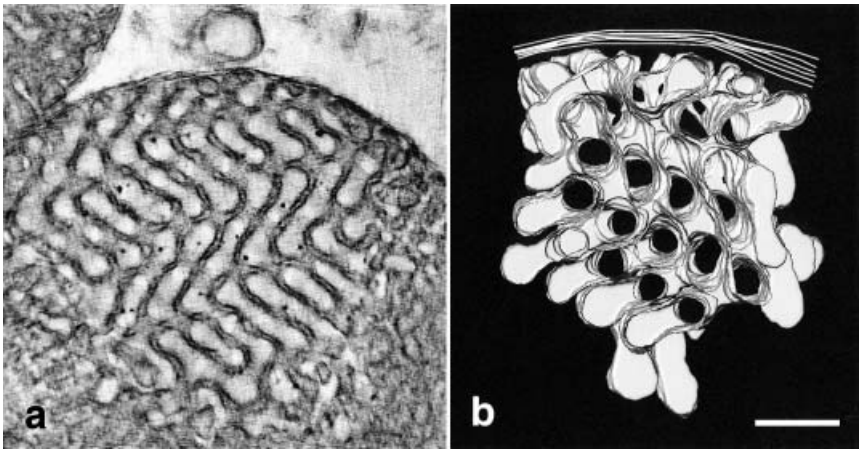

Fig. 1 a, b. Paracrystalline structure of the mitochondrial inner membrane in starved *C. carolinensis* cells. **a** Thin (2.9 nm) slice from a tomographic reconstruction of an amoeba mitochondrion whose cristae have adopted the double-diamond cubic morphology. The empty (white) compartments are the intracristal spaces, whose cross sections in this view (approximately parallel to the [100] lattice direction) have a characteristic herringbone pattern. **b** A surface-rendered model of the inner membranes in this mitochondrion, showing parallel rows of cristae "channels" that span the 145 nm thick volume. These intracristal compartments interconnect with equivalent passageways along the other two principal lattice directions and open into the intermembrane space at numerous points along the inner-membrane periphery. For a full discussion of the three-dimensional geometry of these membranes, see Deng et al. (1999), from which these figures were adapted. Bar: 250 nm

zkowski 1998) and electron tomographic reconstruction (Deng et al. 1999), these periodic membrane structures have been shown to be true cubic morphologies (Fig. 1). However, the mechanisms triggering this change in mitochondrial inner-membrane morphology and its functional consequences are currently unknown.

Relatively little is known about oxidative metabolism in *C. carolinensis* and the changes that might accompany fasting. The few published reports go back over forty years. Respiration was first reported to occur mainly, but not entirely, via a cytochrome oxidase pathway (Pace and Belda 1944b), although cytochrome oxidase was not readily detectable in cell homogenates (Andresen et al. 1951) or in isolated mitochondria (Michejda and Møller 1961). More recently, it was reported that *C. carolinensis* switches from carbohydrate- to lipid-based carbon sources during starvation (Daniel and Breyer 1968). Because the consequences of this switch in energy metabolism are unknown, and because of the seemingly contradictory evidence about cytochrome oxidase-based respiration, we set out to characterize the basic respiratory features of fed and starved *C. carolinensis*. The results described in this paper indicate that fasting leads to development of cyanide-resistant respiration and increased generation of H_2O_2 and reactive oxygen species (ROS). It is proposed that the structural transition in the mitochondrial inner membrane may be, at the same time, a consequence and an integral part of the cell's response to oxidative stress.

Material and methods

Cell culture and harvest

The amoeba, *Chaos carolinensis*, used in this study was originally obtained from Carolina Biological Supply Co. (Burlington, N.C.). The cells have been adapted to mass culture (Prescott 1956) by cultivation in flat-bottomed glass dishes at room temperature with inorganic medium (0.5 mM $CaCl_2$, 0.05 mM $MgSO_4$, 0.16 mM K_2HPO_4, 0.11 mM KH_2PO_4, pH 6.9–7.0) in the presence or absence of their food, the ciliate *Tetrahymena* sp. (bacteria-free culture, also from Carolina Biological Supply Co.). The ciliates were grown separately in 2% proteose peptone media at room temperature. Prior to addition to the amoeba cultures (done weekly), the ciliates were harvested by low-speed centrifugation (1000 rpm) and washed three times in amoeba growth medium to remove all trace of proteose peptone, which is toxic to *C. carolinensis*. Prior to harvesting the amoebae, the cultures were washed gently several times with inorganic medium to remove *Tetrahymena* sp. The amoebae were dislodged from the bottom of the culture dishes by squirting with a washing bottle and placed in tall (500 ml) beakers of growth medium, in which they were allowed to settle by gravity. The supernatant was siphoned off and the clean amoebae were ready for further processing.

Whole-cell respiration

Typically 500–1500 amoebae were suspended in 200 µl of the inorganic growth medium and transferred to a small (3 ml) glass test tube. This tube was fitted with a custom-made microelectrode (MI-730; Microelectrodes Inc., Bedford, N.H.), for the purpose of polarographic measurement of oxygen consumption, which was done at room temperature with continuous stirring. In order to make addi-

tions of KCN, salicyl hydroxamate (SHAM), hydrogen peroxide, etc., to the tube, the electrode seal had to be broken, which introduced an increment of oxygen each time. These offsets are not shown in the traces in Fig. 2.

Detection of alternative oxidase by Western blotting

The same number (40) of fed and 6-day-starved cells were homogenized in 25 µl of growth medium and solubilized in 1% sodium dodecyl sulfate-containing buffer (Laemmli 1970) and heated to 95 °C for 10 min. Electrophoresis was carried out using a Laemmli buffer system (Laemmli 1970) in 10% polyacrylamide gels with a 5% polyacrylamide stacking region. Proteins were electrotransferred to nitrocellulose membranes (Mini-Trans-Blot system; Bio-Rad, Hercules, Calif.) which were blotted (Harlow and Lane 1988) using a 1 : 1000 dilution of an antibody against plant (*Saurumatum guttatum*) alternative oxidase protein, kindly provided by Drs. T. E. Elthon (University of Nebraska), F. E. Sluse (University of Liege, Belgium), and W. Jarmuszkiewicz (Adam Mickiewicz University, Poland). Antibody binding was detected by chemiluminescence (ECL system; Amersham, Piscataway, N.J.).

Fluorescence microscopy

To visualize mitochondria, amoebae were incubated at room temperature, in the dark, for 12 h in inorganic growth medium containing 1 µM MitoTracker Red (Molecular Probes, Eugene, Oreg.), a fluorescent dye that is specifically taken up by metabolically active mitochondria. The cells were washed several times with growth medium prior to microscopic examination. To detect ROS and hydrogen peroxide, amoebae were incubated for up to 2 h with 15 µM 2′,7′-dichlorofluorescein diacetate (H_2DCF-DA) (Molecular Probes). H_2DCF-DA is converted to H_2DCF by intracellular esterases and rapidly oxidized to the highly fluorescent DCF by H_2O_2 and other peroxides. Cells were examined and photographed (1 s exposures) in both fluorescence and differential interference contrast (DIC) modes on a Nikon Optiphot equipped with a Quad Fluor epifluorescence attachment and a ×60 (numerical aperture, 1.4) Planapo objective. Optical sections were captured with a Photometrics PXL 1400 cooled charge-coupled-device camera, processed, and then stored on an SGI workstation using ISee software (Innovision Corp., Durham, N.C.). Selected DIC and epifluorescence digital images were exported from ISee into Adobe PhotoShop (Adobe Systems Inc., Mountain View, Calif.) for subsequent processing.

Spectrofluorometry

Production of H_2O_2 and ROS in cell lysates was detected by spectrofluorometry, using H_2DCF-DA. The same number (80) of washed amoebae (fed or starved for 2 and 8 days) were homogenized on ice in 100 µl of buffer containing 0.25 M sucrose, 10 mM HEPES (pH 7.4), and 1 mM NaEDTA. H_2DCF-DA was added to the lysed cells at a final concentration of 50 µM, followed by other additions (e.g., 1 mM SHAM), immediately before the measurement. Fluorescence intensity was monitored with a Perkin-Elmer (Norwalk, Conn.) LS50B fluorescence spectrometer, using an excitation wavelength of 468 nm and emission wavelength of 519 nm. Readings were made at 20 s intervals for up to 50 min.

Total protein determination

Total cellular protein was determined by the BCA protein assay (Pierce, Rockford, Ill.), using bovine serum albumin as a standard.

Chemicals

KCN and SHAM were obtained from Sigma Chemicals (St. Louis, Mo.) and dissolved in inorganic growth medium and 95% ethanol, respectively, at a concentration of 100 mM (stock solutions).

Results

Changes in respiratory activity of C. carolinensis during fasting

When food sources are withdrawn, Chaos cells visibly shrink to a small fraction of their usual size (1–3 mm in length). This loss of cell volume is accompanied by a decrease in protein content, from an average of 0.41 µg/cell to 0.30 µg/cell and 0.21 µg/cell after 2 and 7 days of fasting, respectively. Whole-cell polarography was used to monitor the basal respiratory rates of Chaos cells and the sensitivity of this respiration to cyanide. The kinetics of oxygen consumption by suspensions of fed cells and cells starved for 1 and 7 days are shown in Fig. 2 A. The specific rate of respiration of fed cells was, typically, 3 pmol of O_2 per min per cell. Basal respiration per cell was found to decrease with fasting, e.g., by 13% and 57% after 1 and 7 days of fasting, respectively, in the experiments of Fig. 2. The latter decrease is similar to that reported by Pace and Belda (1944a) for Chaos cells starved for 7 days (66%). However, because cellular protein content decreased during starvation, the corresponding specific respiratory rates (expressed per mg of cell protein) actually increased for cells starved for 1 day and decreased only with prolonged starvation. In the experiments of Fig. 2 A, the specific rates of O_2 consumption were 7.3, 8.7, and 6.2 nmol/min·mg of protein for fed cells and cells starved 1 and 7 days, respectively.

While respiration of fed Chaos cells was fully inhibited by 1 mM KCN, inhibition by KCN was only partial (80%) with cells fasted for 1 day (Fig. 2 A). Likewise, the respiration of starved cells, but not fed cells, was found to be inhibited by SHAM, an inhibitor of the alternative oxidase (AOX) found in plants, fungi, and protists (Moore and Siedow 1991). The combined effect of SHAM and KCN on the respiration of 1.5-day-starved amoebae was full inhibition of O_2 consumption (Fig. 2 B). These results indicate that two respiratory pathways are active in starved cells, the usual cyanide-sensitive pathway, which presumably uses cytochrome oxidase as the terminal electron donor to O_2, and a second that involves a cyanide-resistant, SHAM-sensitive AOX.

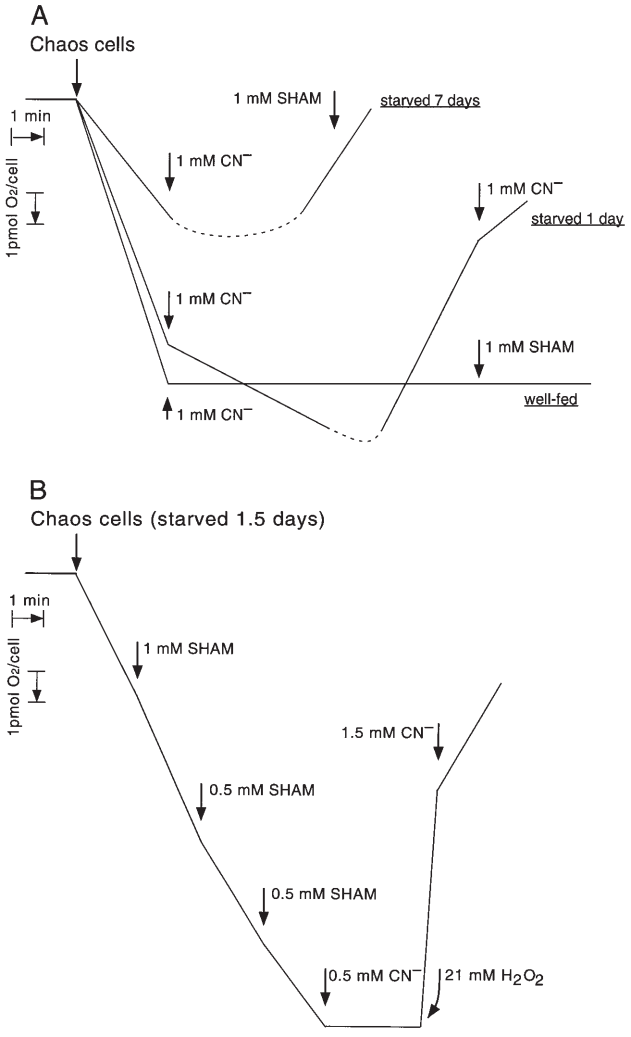

Fig. 2 A, B. Whole-cell respiration of *C. carolinensis* cells and detection of catalase activity. **A** Polarographic measurements from fed, 1-day-starved, and 7-day-starved cells, indicating relative effects of 1 mM KCN on oxygen consumption. Dashed lines indicate the passing of several minutes prior to the upturn in the curves, corresponding to oxygen production, presumably due to endogenous catalase activity (see text). **B** Cumulative effects of SHAM and KCN on respiration of cells starved for 1.5 days. Following full respiratory inhibition, excess H_2O_2 was added to determine maximum catalase activity

Western blot analysis was performed to determine whether a plantlike alternative oxidase protein could be detected in Chaos cells. The data (not shown) was inconclusive. Using an antibody against plant AOX, bands were observed for fed and 6-day-starved cells at M_r of about 38, as expected for the AOX protein. However, these bands were not significantly stronger than numerous other, presumably nonspecific bands in the same blots. If, in fact, both fed and starved cells contain AOX protein, the respiratory measurements described above suggest that AOX activity is normally latent in *C. carolinensis* and activated by fasting.

Cyanide-induced oxygen production

It proved to be difficult to measure cyanide inhibition of cells starved for 7 days because of a highly unusual phenomenon, namely, a spontaneous generation of O_2 following KCN addition (Fig. 2 A). A similar effect was observed with cells starved for only 1 day, after prolonged incubation in the presence of KCN (Fig. 2 A). This O_2 production was not seen with buffer alone (no cells) or with fed cells. Rates of O_2 generation in starved cells were between 5 and 10 nmol/min·mg of protein.

The source of this O_2 generation is puzzling. It was found that addition of H_2O_2 to fed (not shown) or starved cells (Fig. 2 B) resulted in very rapid rates of O_2 production (50–200 nmol/min·mg of protein), indicating that Chaos cells have high levels of endogenous catalase activity. This raises the possibility that the remarkable O_2 production exhibited by starved Chaos cells might result from reaction of catalase with an internal pool of H_2O_2, somehow released by the action of KCN:

$$[H_2O_2]_{pool} \xrightarrow{KCN} [H_2O_2]_{cytosol} \xrightarrow{catalase} H_2O + 1/2\ O_2.$$

Both the spontaneous and peroxide-induced O_2 production were partially inhibited when the external concentration of KCN (an inhibitor of catalase as well as cytochrome oxidase) was raised to 2 mM (Fig. 2 A, B), which is consistent with at least some of the observed O_2 generation being catalase-based. This raises the question of whether H_2O_2 is produced in larger quantities and stored in internal compartments by starving Chaos cells.

Elevated generation of H_2O_2 and ROS by C. carolinensis during fasting

The production of H_2O_2 and reactive O_2 species by fed and starved Chaos cells was measured with the dye H_2DCF-DA. When cell lysates were incubated with H_2DCF-DA, the rate of increase of fluorescence intensity (per mg of cellular protein) was found to increase progressively with time of fasting (Fig. 3). This indicates that starvation of *C. carolinensis* leads to increased rates of H_2O_2 and ROS generation. KCN did not have a noticeable effect on H_2O_2 and ROS pro-

duction by the lysates, but addition of SHAM tended to stimulate these rates in starved cells.

When intact Chaos cells were incubated with H_2DCF-DA and imaged by epifluorescence microscopy, fluorescence intensity was greatest in large (20–50 µm) vacuoles distributed throughout the cytoplasm (Fig. 4 E, F). The distribution of fluorescence intensity arising from H_2DCF-DA was very different from that obtained with MitoTracker Red (Fig. 4 A–D), which is taken up by energized mitochondria. Localization of H_2DCF-DA fluorescence to cytosolic vacuoles is consistent with storage of H_2O_2 and/or ROS inside these compartments. Cytoplasmic motion and the heterogeneous distribution of H_2DCF-DA fluorescence, however, prevented reliable quantitation of differences in fluorescence intensity between different cells (e.g., fed vs. starved) or within the same cells following addition of respiratory inhibitors.

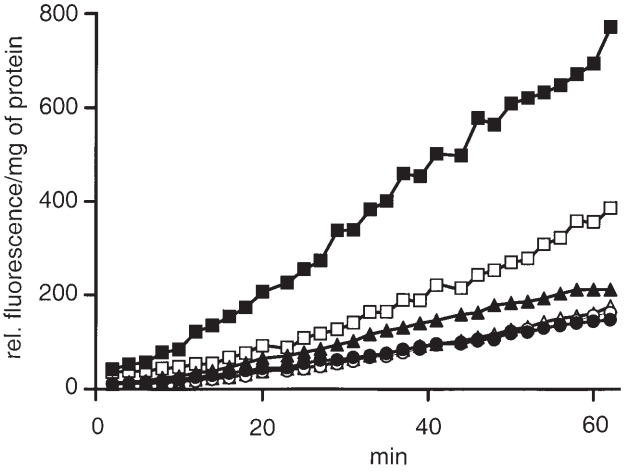

Fig. 3. Time course of H_2O_2 and ROS generation in lysates of fed (circles) and starved (triangles, 2 days; squares, 8 days) *C. carolinensis* cells, measured by spectrofluorimetry using the dye H_2DCF-DA. ○, △, □ Experiments without SHAM. ●, ▲, ■ Experiments with addition of 1 mM SHAM

Discussion

Withdrawal of food organisms from cultures of *C. carolinensis* leads to progressive loss of cell mass and volume and a dramatic structural change in the mitochondrial inner membrane to cubic morphology. Total respiration per cell decreases markedly (by two thirds) after one week of fasting, but specific respiratory rates (per mg of cell protein) drop only modestly (about 15%). Starvation is accompanied by development of KCN-insensitive, SHAM-sensitive respiration, associ-

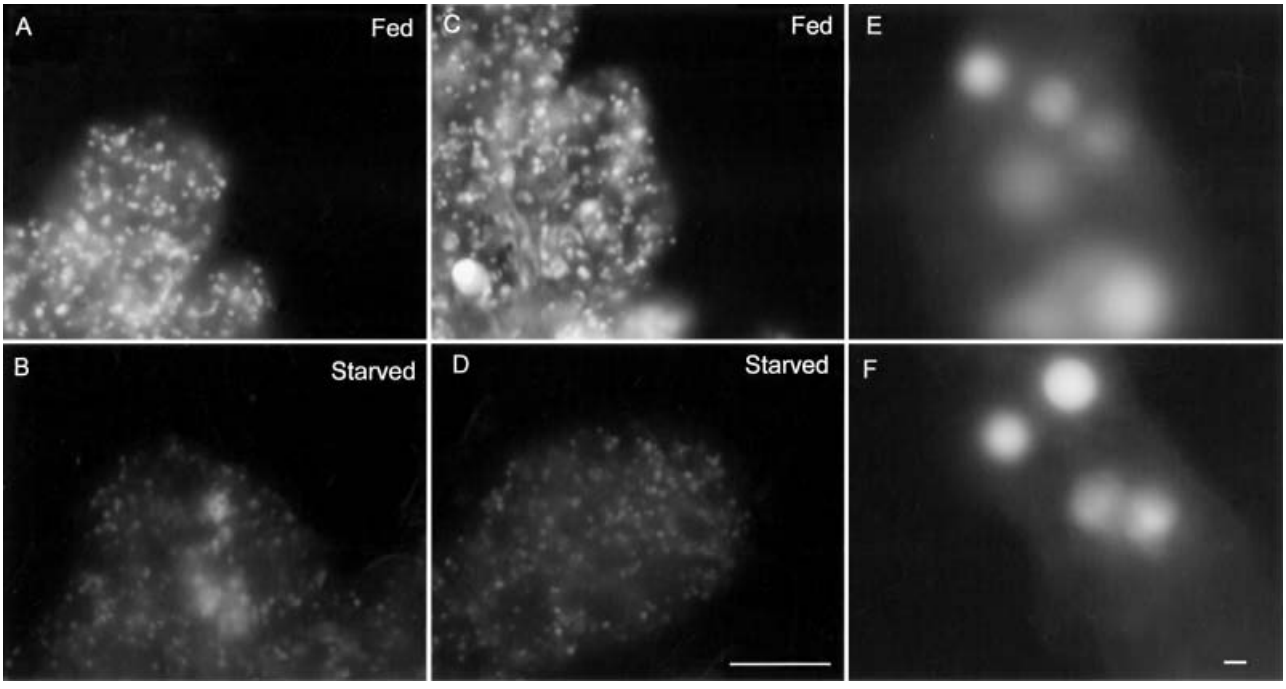

Fig. 4 A–D. Fluorescence microscopy of *C. carolinensis* cells to detect mitochondrial membrane potential and H_2O_2 and ROS production. **A–D** Images of fed (**A** and **C**) and 7-day-starved (**B** and **D**) cells preincubated with MitoTracker Red, which is taken up and fluoresces in energized mitochondria. **E** and **F** Images of starved cells preincubated with H_2DCF-DA, which fluoresces in response to peroxides and oxygen radicals. Bars: 20 µm

ated with activation of an AOX pathway. The fraction of KCN-insensitive respiration observed after one day of fasting (20%) is similar to the increase in specific respiratory activity over the same period (19%). Thus, assuming that the bulk of O_2 consumption by these cells is due to mitochondrial respiratory activity, it appears that this activity is not seriously diminished by transition of the cristae to cubic morphology. The time course of accumulation of MitoTracker Red by Chaos mitochondria was found to be consistently slower for starved vs. fed cells (compare Fig. 4 A, C with B, D). However, it was undetermined whether this was due to decreased mitochondrial membrane potential or to slower uptake of the dye by the starved cells (see Prusch 1981).

Besides the development of KCN-resistant respiration, the other major change in oxidative metabolism during starvation of *C. carolinensis* is increased generation of H_2O_2 and ROS. There are at least two likely sources of elevated H_2O_2 and ROS: increased mitochondrial generation of $O_2^{\bullet-}$, followed by its dismutation to H_2O_2 and O_2; and increased peroxisomelike, fatty acid β-oxidation activity, which would directly generate H_2O_2. It seems reasonable that fatty acid oxidation might be stimulated in the amoebae when they begin to catabolize their lipid stores during starvation (Daniel and Breyer 1968). For example, it is well-documented that fasting in rats is accompanied by stimulation of peroxisomal as well as mitochondrial and microsomal pathways of fatty acid oxidation (McGarry and Foster 1980, Orellana et al. 1993). Whatever the source of the elevated H_2O_2 and ROS, prolonged oxidative stress can be expected to have serious consequences in terms of damage to DNA, proteins, and membrane lipids (e.g., Halliwell and Gutteridge 1999). However, *C. carolinensis* appears to have several protective mechanisms in place to minimize this damage. These include high catalase activity (Fig. 2 B) and sequestration of H_2O_2 (and possibly other oxidative species) in intracellular vacuoles. As already noted, release of stored H_2O_2 from these internal compartments into the cytosol (where it can react with catalase) may explain the unusual O_2 production observed when starved cells are treated with KCN. The effect of KCN may be simply to deplete cellular [ATP] below the level needed to sequester H_2O_2 in the vacuoles. The alternative oxidase activated in *C. carolinensis* during fasting might represent a third protective mechanism since SHAM (an AOX inhibitor) increased production of H_2O_2 and ROS in starved amoebae. Several studies indicate that the AOX pathway in plants serves as an electron shunt to reduce mitochondrial oxygen radical formation during high respiratory activity (Purvis and Shewfelf 1993, Skulachev 1996, Wagner and Moore 1997, Maxwell et al. 1999). In the case of fasting amoebae, it is not obvious why an AOX shunt would be protective, since respiration rates are lower than those of fed cells (although the reduction in specific respiratory rate is, in fact, modest as explained above). One possibility is that the respiratory chain downstream of ubiquinone (the electron donor to AOX) becomes leaky to electrons with cumulative oxidative damage to mitochondrial membrane proteins and lipids. If so, reducing electron flux through complexes III and IV by shunting electrons to AOX would help to slow the production of $O_2^{\bullet-}$.

The transition of mitochondrial cristae to cubic morphology might itself be a protective mechanism against oxidative stress. The inner mitochondrial membrane of a fed amoeba has long, narrow tubular invaginations that are characteristic of protozoan cristae (Munn 1974). Conversion of these narrow tubes to an elaborate network of enlarged and interconnected compartments (Fig. 1) could expedite the efflux of H_2O_2 (produced by enzymatic dismutation of $O_2^{\bullet-}$) out of the mitochondria and into the cytoplasmic vacuoles, which are often in close proximity to mitochondria. The change in inner-membrane shape might also facilitate the exit of $O_2^{\bullet-}$ itself, since experiments with rat liver mitochondria indicate that superoxide generated by the respiratory chain is released into the intermembrane or intracristal space, as well as into the matrix (Han et al. 2001). The change in membrane curvature that accompanies the cubic structural transition also might serve to reduce peroxidative damage to the inner membrane. Li et al. (2000) report that phosphatidyl choline in small liposomes (average radius, 12.5 nm) is more susceptible to attack by water-soluble oxidants than it is when incorporated into larger membrane vesicles (average radius, 53.5 nm). The enhanced susceptibility to peroxidation of this phospholipid, a common constituent of mitochondrial membranes, likely reflects the ease with which oxidants can penetrate the more loosely packed surface of lipid vesicles with a smaller radius of curvature. The cubic membranes of mitochondria in starved *C. carolinensis* (Fig. 1) form a continuously curved surface with a radius of curvature at any point of about 50 nm, which is considerably larger than the radius of the cristae tubes

found in fed amoebae (about 20 nm). The curvature of the cubic mitochondrial membranes is similar to that of the large vesicles found by Li et al. (2000) to resist peroxidative attack, while the tubular membranes have a curvature much closer to that of the smaller, more readily peroxidized liposomes. Finally, the reshaping of the inner membrane might even accelerate the conversion of $O_2^{\bullet-}$ to H_2O_2. There are reports of nonenzymatic superoxide dismutase activity in mitochondria associated with direct reduction of ROS by protons at the inner membrane (Guidot et al. 1995). The cubic transition of the inner membrane might enhance any nonenzymatic superoxide dismutase activity by creating an easily accessed continuum of catalytic membrane surfaces.

The correlated appearance of cubic mitochondrial membranes with the onset of oxidative stress in fasting amoebae raises the possibility that the structural transition itself might be triggered by a change in membrane composition. For example, cardiolipin, a predominant inner-membrane lipid, is especially susceptible to peroxidation due to the high degree of desaturation of its acyl chains (e.g., Paradises et al. 1998). Loss of cardiolipin or accumulation of peroxidized phospholipid products in the mitochondrial membrane could be expected to change lipid packing and so alter membrane curvature. Analyses of the lipid composition of fed and starved Chaos cells are in progress (Y. Deng, S. Kohlwein, G. Gogg-Fassolter, M. Hayn, and C. Mannella unpubl. results).

Landh (1995, 1996) has extensively surveyed the naturally occurring cubic membrane systems, and most notably, a great many are associated with processes involving elevated ROS. Examples include mitochondria and endoplasmic reticulum of photoreceptor and developing germ cells, thylakoid membranes of some plant chloroplasts, and endomembranes of neoplastic and virus-infected cells. A specialized cubic membrane structure in which ROS generation is central to function is the photosome. This is a specialized region of endoplasmic reticulum in a marine annelid that is associated with intense ROS generation and chemiluminescence (Bassot and Nicolas 1995). Thus, it is possible that the transition of biological membranes to cubic morphologies may be a general response to oxidative stress. If so, the conditional cubic membrane system in Chaos mitochondria that is inducible by starvation may be a valuable model for studying oxidative stress mechanisms, which underlie a wide variety of human diseases.

Acknowledgments

We acknowledge use of the Wadsworth Center's Video Light Microscopy and Biochemistry core facilities. We also thank Drs. W. Jarmuszkiewicz (Adam Mickiewicz University, Poznan, Poland) and T. E. Elthon (University of Nebraska) for providing the antibody against plant AOX, and Drs. F. Sluse (University of Liege, Belgium) and T. Landh (Camurus Lipid Research Foundation) for helpful discussions in the course of this work. Special thanks also go to A. Shih (Albany Medical College), R. Cole (Wadsworth Center), and M. Marko (Wadsworth Center) for important technical assistance. The work is supported by Camurus Lipid Research Foundation (Y.D.) and Austrian Science Fund (project F706) (S.D.K.).

References

Andresen N, Engel FR, Holter H (1951) Succinic dehydrogenase and cytochrome oxidase in *Chaos chaos*. C R Lab Carlsberg Ser Chim 27: 408–420

Bassot J-M, Nicolas M-T (1995) Bioluminescence in scale-worm photosomes: the photoprotein polynoidin is specific for the detection of superoxide radicals. Histochem Cell Biol 104: 199–210

Daniel EW, Breyer EP (1968) Starvation effects on the ultrastructure of amoeba mitochondria. Z Zellforsch 91: 159–169

Deng Y, Mieczkowski M (1998) Three-dimensional periodic cubic membrane structure in the mitochondria of amoebae *Chaos carolinensis*. Protoplasma 203: 16–25

– Marko M, Buttle KF, Leith A, Mieczkowski M, Mannella CA (1999) Cubic membrane structure in amoeba (*Chaos carolinensis*) mitochondria determined by electron microscopic tomography. J Struct Biol 127: 231–239

Engström S (1990) Drug delivery from cubic and other lipid-water phases. Lipid Technol 2: 42–45

Guidot DM, Repine JE, Kitlowski AD, Flores SC, Nelson SK, Wright RM, McCord JM (1995) Mitochondrial respiration scavenges extramitochondrial superoxide anion via a nonenzymatic mechanism. J Clin Invest 96: 1131–1136

Halliwell B, Gutteridge JMC (1999) Free radicals in biology and medicine. Oxford University Press, New York

Han D, Williams E, Cadenas E (2001) Mitochondrial respiratory chain-dependent generation of superoxide anion and its release into the intermembrane space. Biochem J 353: 411–416

Harlow E, Lane D (1988) Antibodies: a laboratory manual. Cold Spring Harbor Laboratory, Cold Spring Harbor, NY

Hyde ST (1996) Bicontinuous structure in lyotropic liquid crystals and crystalline hyperbolic surfaces. Curr Opin Solid State Mater Sci 1: 653–662

Laemmli UK (1970) Cleavage of structural proteins during the assembly of the head of bacteriophage T4. Nature 227: 680–685

Landh T (1995) From entangled membranes to eclectic morphologies: cubic membranes as subcellular space organizers. FEBS Lett 369: 13–17

– (1996) Cubic cell membrane achitectures: taking another look at membrane bound cell spaces. PhD thesis. University of Lund, Lund, Sweden

Larsson K (1989) Cubic lipid-water phases: structures and biomembrane aspects. J Phys Chem 93: 7304–7314

Li Q-T, Yeo MH, Tan BK (2000) Lipid peroxidation in small and large phospholipid unilamellar vesicles induced by water-soluble free radical sources. Biochem Biophys Res Commun 273: 72–76

Maxwell DP, Wang Y, Mcintosh L (1999) The alternative oxidase lowers mitochondrial reactive oxygen production in plant cells. Proc Natl Acad Sci USA 96: 8271–8276

McGarry JD, Foster DW (1980) Regulation of hepatic fatty acid oxidation and ketone body production. Annu Rev Biochem 49: 395–420

Michejda J, Møller KM (1961) Respiratory enzymes in amoeba *Chaos chaos*. V Int Congr Biochem 23: Abst 1054

Moore AL, Siedow JN (1991) The regulation and nature of the cyanide-resistant alternative oxidase of plant mitochondria. Biochim Biophys Acta 1059: 121–140

Munn EA (1974) The structure of mitochondria. Academic Press, London

Orellana M, Fuentes O, Valdes E (1993) Starvation effect on rat kidney peroxisomal and mitochondrial fatty acid oxidation: a comparative study between liver and kidney. FEBS Lett 322: 61–64

Pace DM, Belda WH (1944a) The effect of food content and temperature on respiration in *Pelomyxa carolinensis* Wilson. Bio Bull 86: 146–153

– – (1944b) The effects of potassium cyanide, potassium arsenite, and ethyl urethane on respiration in *Pelomyxa carolinensis*. Biol Bull 87: 138–144

Paradises G, Ruggiero FM, Petrosillo G, Quagliariello E (1998) Peroxidative damage to cardiac mitochondria: cytochrome oxidase and cardiolipin alterations. FEBS Lett 424: 155–158

Prescott DM (1956) Mass and clone culturing of *Amoeba proteus* and *Chaos chaos*. C R Lab Carlsberg Ser Chim 30: 1–12

Prusch RD (1981) Bulk solute extrusion as a mechanism conferring solute uptake specificity by pinocytosis in *Amoeba proteus*. Science 213: 668–670

Purvis AC, Shewfelf RL (1993) Does the alternative pathway ameliorate chilling injury in sensitive plant tissues? Physiol Plant 88: 712–718

Skulachev VP (1996) Role of uncoupled and non-coupled oxidations in maintenance of safely lower levels of oxygen and its one-electron reductants. Q Rev Biophys 29: 169–202

Wagner AK, Moore AL (1997) Structure and function of the plant alternative oxidase: its putative role in the oxygen defense mechanism. Biosci Rep 17: 319–333